THE POTENTIAL OF DUAL-WAVELENGTH TERRESTRIAL LASER SCANNING IN 3D CANOPY FUEL MOISTURE CONTENT MAPPING

A. Elsherif [1, 2, *], R. Gaulton [1], J. P. Mills [1]

[1] School of Engineering, Newcastle University, Newcastle upon Tyne, UK - (a.m.a.elsherif2, rachel.gaulton, jon.mills)@newcastle.ac.uk
[2] Faculty of Engineering, Tanta University, Tanta, Egypt

Commission III, WG III/5

KEY WORDS: Ground-based lidar, fuel moisture content, forest wildfires, vegetation

ABSTRACT:

Terrestrial laser scanning (TLS) instruments have been widely utilized in measuring vegetation canopy structural parameters, being capable of providing high density point clouds. However, less attention has been paid to using TLS intensity data in estimating vegetation biochemical attributes, and calculating water status metrics, that can help in early detection of vegetation stress and risk of wildfire. Water status metrics, such as the leaf Equivalent Water Thickness (EWT) and the Fuel Moisture Content (FMC), are being commonly estimated from optical remote sensing data. However, such estimates mainly reflect the water status of canopy top and ignore the vertical heterogeneity of water content distribution within the canopy. The estimates are also affected by canopy structure and understory reflectance. Such limitations can potentially be addressed using TLS intensity data, as observations are performed in three dimensions (3D). This study therefore investigated the potential of using dual-wavelength TLS intensity data to estimate FMC in 3D. The calculated Normalized Difference Index (NDI) of 808 nm near infrared and 1550 nm shortwave infrared wavelengths was found to be correlated to FMC at leaf level for four different tree species. The correlation was moderate, and the relationships were not consistent between species. NDI was subsequently used to estimate FMC at canopy level in seven trees in a small tree plot with an average error < 5 %. The 3D estimates of FMC revealed vertical heterogeneity in all trees measured, which varied between species and also between trees from the same species.

1. INTRODUCTION

Terrestrial Laser Scanning (TLS) instruments can measure the three dimensional (3D) coordinates of points in the surrounding environment with high speed and accuracy, providing dense point clouds that include high-resolution information about the structure of the scanned objects. As a result, TLS instruments have been widely utilized in measuring vegetation canopy biophysical attributes, including but not limited to: tree height, diameter at breast height, forest biomass, vertical forest canopy foliage profile, directional gap fraction, and leaf area index (Ramirez et al., 2013; Takeda et al., 2008). Furthermore, TLS point clouds include intensity imagery in which the backscattered energy for each point is recorded. Intensity data can be linked to scanned target apparent reflectance (Penasa et al., 2014) and used to provide 3D estimates of vegetation biochemical characteristics (Eitel et al., 2010). Such 3D estimates can help in better understanding, and even overcoming, the limitations associated with 2D estimates generated from spaceborne and airborne remote sensing data. Such limitations include ignoring the vertical heterogeneity in vegetation canopy biochemical and biophysical characteristics, as it is challenging to measure and account for in the estimation models (Valentinuz and Tollenaar, 2004). In addition, the sub-canopy soil and vegetation affect the accuracy of the vegetation canopy biochemical characteristics estimation (Eitel et al., 2010). Such limitations can be addressed by performing the estimations in three dimensions.

There have been several successful attempts in recent years to utilize TLS intensity data in the estimation of vegetation biochemical characteristics. This has included measuring leaf nitrogen content (Du et al., 2016; Eitel et al., 2014a; Eitel et al., 2014b; Eitel et al., 2011; Wei et al., 2012), leaf chlorophyll content (Eitel et al., 2010; Hakala et al., 2015; Li et al., 2016; Nevalainen et al., 2014), and leaf Equivalent Water Thickness (EWT) (Elsherif et al., 2018; Gaulton et al., 2013; Junttila et al., 2018; Junttila et al., 2016; Zhu et al., 2015; Zhu et al., 2017). EWT, defined as the amount of water in a given leaf area (Yilmaz et al., 2008), can generally be linked to the Fuel Moisture Content (FMC), which is the amount of water in a leaf divided by the leaf dry weight (Yebra et al., 2008). FMC is linked to the potential risk of fire ignition and propagation (Viegas et al., 1992), in addition to the fire spread rate (Nelson Jr, 2001). Thus, It has been widely used in wildfire modelling and early detection of wildfire risk (Danson and Bowyer, 2004). The recent successful estimation of EWT using TLS data opens the door to estimating FMC using similar approaches.

The main aim of this study was to investigate the potential of using the Normalized Difference Index (NDI) of 808 nm near infrared and 1550 nm shortwave infrared wavelengths, as utilized in the Leica P20 and P50 TLS instruments respectively, in estimating FMC of seven tree canopies from four different species. Additional aims included studying the vertical variation of FMC within tree canopies and between species, as well as between different trees from the same species.

* Corresponding author

2. METHODS

2.1 TLS instrumentation and calibration

The Leica P20 and P50 instruments are time-of-flight, pulsed TLS systems, operating at 808 nm near infrared and 1550 nm shortwave infrared wavelengths respectively. They are capable of acquiring up to one million points per second and have a highest point spacing resolution of 0.8 mm at 10 m. The laser beam diameter at exit is 2.8 mm and 3.5 mm for the P20 and the P50 instruments, respectively. The beam divergence is 0.20 mrad for the P20 and 0.23 mrad for the P50. The similarities between the two instruments in terms of their chassis and scanning mechanism provide the potential for high registration accuracy between point clouds acquired from common scan stations, despite the differences in laser beam exit location and divergence, as discussed in Elsherif et al. (2018). The maximum range of the P20 is 120 m at 18 % reflectivity, while the P50 has a maximum range of 1 km at 80 % reflectivity (120 m at 8 % reflectivity). Calibration of the P20 intensity data to retrieve apparent reflectance is described in Elsherif et al. (2018). In a similar manner, and using the same concept, the P50 intensity data was calibrated in this study using a multi-step SphereOptics Zenith Lite Diffuse reflectance target (actual reflectance of 5.5 %, 20.5 %, 47.7 % and 91.8 %). The multi-step target was scanned at various ranges from the instrument, starting at 2 m and ending at 22 m, with incremental steps of 1 m. Polynomial functions that described the intensity-range and intensity-reflectance relationships of the instrument were then fitted to the scan data.

2.2 Study area and TLS data processing

Data collection took place in a tree plot (35 m × 35 m) in Exhibition Park, Newcastle upon Tyne, UK (54.98° N, 1.62° W). One scanning position was set in the centre of the plot, and seven trees from four different species were scanned. The tree species included: two *Sorbus intermedia* (Swedish Whitebeam), one *Fagus sylvatica* (Beech), two *Fraxinus excelsior* (Ash), and two *Ilex aquifolium* (Holly). The trees were scanned using both the P20 and the P50 instruments from a single scanning position, mounted consecutively on the same tripod. The scans took place on 22nd October 2018, while the leaves were senescing. Three Leica black and white registration targets were placed in the scene for co-registration of the P20 and P50 point clouds and full-hemisphere scans (360° × 270°) were conducted with a common resolution of 3 mm at 10 m.

The point clouds were aligned using Leica Cyclone version 9.1 prior to the intensity being calibrated to apparent reflectance on a point-by-point basis, using the models described in Section 3.1. A NDI point cloud was generated by applying Equation (1) on a point-by-point basis and individual trees were then manually extracted. The NDI – FMC relationship of each species, determined at leaf level (Section 3.2), was applied to the trees according to their species and FMC point clouds were generated.

$$NDI = (P20_R - P50_R) / (P20_R + P50_R) \quad (1)$$

where $P20_R$ = reflectance from the P20 instrument
$P50_R$ = reflectance from the P50 instrument

2.3 Leaf sampling

Leaf samples were physically collected immediately following scanning of the tree plot. The total number of leaf samples collected was 38. Table 1 provides the number of leaf samples collected for the purpose of both building the FMC estimation models and validating the estimation.

Species	FMC model	Validation
Swedish Whitebeam	5	5
Beech	5	4
Ash	5	5
Holly	4	5

Table 1. Number of leaf samples collected.

Samples for building the FMC estimation models were collected randomly. Samples for validation were collected from a small volume, approximately 0.5 m × 0.5 m × 0.5 m, in a single tree from each species. Fresh weight (FW) of each sample was measured immediately on collection using a precise scale (0.001g division). Dry weight (DW) was measured after drying the samples in an oven for 72 hours at 60 °C. The FMC of each sample was calculated as:

$$FMC\ (\%) = ((FW - DW) / DW) \times 100 \quad (2)$$

Samples for building the FMC estimation models were scanned by both the P20 and P50 at a range of 7 m, immediately after measuring their FW. NDI was calculated for each leaf according to Equation (1) after calibrating the intensity to apparent reflectance, using the calibration models described in Section 3.1. NDI was plotted against the corresponding FMC to determine the NDI – FMC estimation model for each species.

3. RESULTS AND DISCUSSION

3.1 Intensity calibration model

The results revealed that the intensity – range relationship for the P50 instrument deviates from the laser equation (Figure 1). The laser equation (Höfle and Pfeifer, 2007) states that the magnitude of intensity is inversely proportional to the range squared. Such deviation was a result of the instrument being equipped with near distance intensity reducer and far distance intensity amplifier, as discussed in Elsherif et al. (2018) for similar instruments.

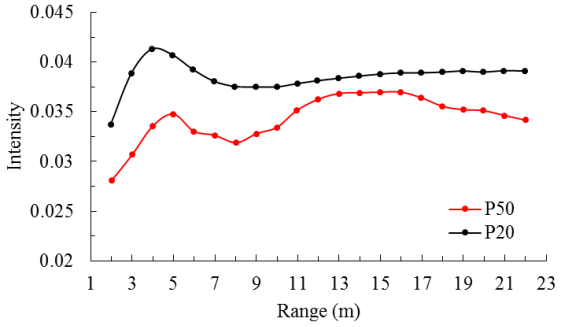

Figure 1. Intensity – range relationships for the P50 and the P20 TLS instruments.

In order to provide an optimal fit, two polynomial functions were fitted to the intensity – range relationship to be used in the calibration. The functions can be described as follows:

$$I = -0.00035 \times R_a^2 + 0.00482 \times R_a + 0.01973, \text{ for } R_a < 5m \quad (3)$$

$$I = -2.3 \times 10^{-8} \times R_a^6 + 1.8 \times 10^{-6} \times R_a^5 - 5.5 \times 10^{-5} \times R_a^4 + 0.0008 \times R_a^3 - 0.0057 \times R_a^2 + 0.0171 \times R_a + 0.0204, \text{ for } R_a > 5m \quad (4)$$

where I = the intensity from the polynomial function
R_a = the range

The intensity – reflectance relationship can be described as:

$$P50_R = 27.1214 \times R_a^2 + 11.9837 \times R_a - 0.0034 \quad (5)$$

where $P50_R$ = reflectance from the P50 instrument

3.2 Leaf level

The highest observed FMC was observed in Ash leaf samples (189 %), followed by Holly leaf samples (168 %). The Beech leaf samples had a lower FMC (138 %), whilst FMC observed in the Swedish Whitebeam samples was the lowest (126 %). Moderate linear correlation was observed between NDI and FMC for all species (R^2 = 0.53, 0.51, 0.60 and 0.45 for Swedish Whitebeam, Beech, Ash and Holly, respectively). NDI and FMC were found to be directly proportional for Swedish Whitebeam and Holly species, but inversely proportional for Ash and Beech (Figure 2).

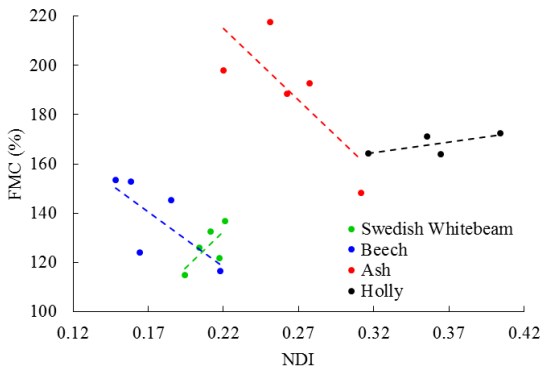

Figure 2. The determined NDI – FMC relationships.

The NDI – FMC relationship was found to be species-dependent and it was not possible to fit a pooled, species-independent FMC estimation model. This observed variation in the NDI – FMC relationships between species was caused by the difference in dry matter content (Leaf Mass per Area, LMA) between them, as FMC is sensitive to the change in LMA (Riaño et al., 2005; Yebra et al., 2008). Although NDI of near- and shortwave-infrared wavelengths was successfully used to estimate EWT, being insensitive, to an extent, to the change in LMA (Elsherif et al., 2018; Gaulton et al., 2013), using it to estimate FMC in a similar manner would be more challenging. The variation in LMA between species, and also within each species, must be accounted for. This agreed with the findings of Ceccato et al. (2001), reporting that EWT and FMC are not always directly related, as they are two different ways to define vegetation water content, and observing inverse relationship between them in some species, as a result of the LMA effects. The species-specific NDI – FMC relationships can be described as:

$$FMC\ (\%) = 581.46 \times NDI + 4.58, \text{ for Swedish Whitebeam} \quad (6)$$

$$FMC\ (\%) = -445.18 \times NDI + 216.27, \text{ for Beech} \quad (7)$$

$$FMC\ (\%) = -580.57 \times NDI + 342.55, \text{ for Ash} \quad (8)$$

$$FMC\ (\%) = 83.86 \times NDI + 137.86, \text{ for Holly} \quad (9)$$

3.3 Canopy level

At canopy level, the sections from which leaf samples for validation were collected were extracted from the FMC point clouds of the trees. The estimated FMC was compared to the actual FMC of leaf samples and the relative errors in the estimation were calculated (Table 2). The errors in the FMC estimations were < 8 % in the four trees used for validation, with the average error in the estimation being 4.5 %.

Species	Actual FMC (%)	Estimated FMC (%)	Relative error (%)
Swedish Whitebeam	146.8	135.5	-7.7
Beech	137.5	128.6	-6.4
Ash	189.7	186.4	-1.6
Holly	166.1	169.8	2.2

Table 2. Relative errors in the FMC estimations.

3D FMC point clouds were generated for six out of the seven trees in the plot, as the Beech tree was partially occluded by two other trees. Figure 3 shows the 3D FMC point cloud for Swedish Whitebeam tree 1 as an example. The FMC point clouds revealed a significant difference between leaf and wood, and also showed vertical heterogeneity in FMC distribution within canopy.

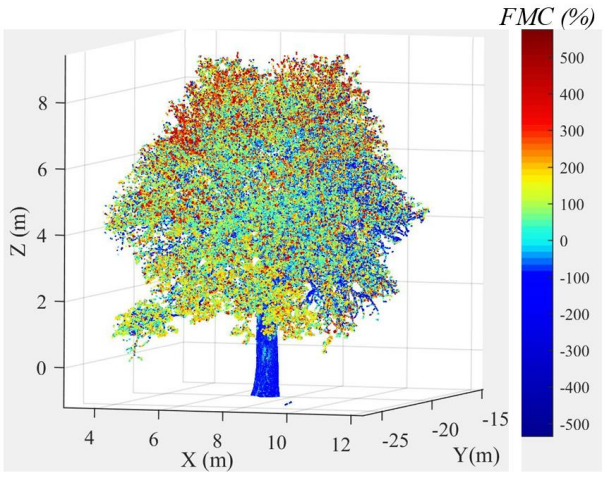

Figure 3. 3D FMC point cloud of Swedish Whitebeam tree 1, showing a heterogeneity in FMC distribution within canopy, and difference between FMC of foliage and wood.

3.4 FMC vertical profiles

To further study the FMC heterogeneity, each FMC point cloud, after manually removing the points corresponding to woody

materials, was divided into a number of horizontal layers, each 1 m thick, and the FMC was calculated for each layer. FMC of layers was plotted against height to produce a FMC vertical profile for each tree, as shown in Figure 4. FMC vertical profiles concurred with the visual inspection of point clouds and revealed some vertical variation in all trees. The vertical profiles of FMC varied between species, and also showed some variation between the two trees from each species. For Swedish Whitebeam trees (Figure 4a), the trees displayed hour-glass shaped FMC distribution, with the lowest FMC being located in the middle of the canopy, which was more obvious in tree 1 than in tree 2. The two trees had similar FMC in upper canopy (layers > 6 m), whilst tree 1 had a higher FMC in lower canopy than tree 2. Overall, tree 1 had 28 % higher average FMC that tree 2 (138 % and 108 %, respectively).

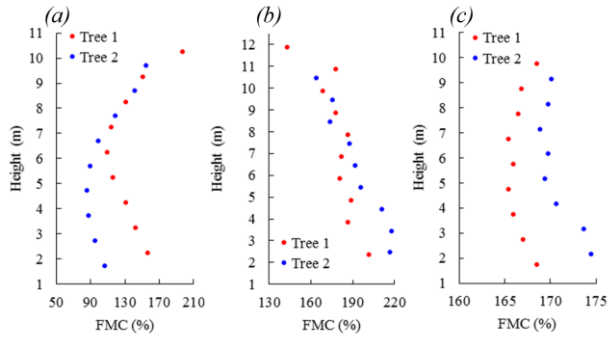

Figure 4. FMC vertical profile for six trees in the plot: (a) Swedish Whitebeam trees 1 and 2, (b) Ash trees 1 and 2, and (c) Holly trees 1 and 2.

For Ash trees (Figure 4b), the two trees had similar FMC in upper canopy (layers > 7 m), while tree 2 had higher FMC in lower canopy than tree 1. However, the difference in the mean FMC between the trees was less significant than that in the Swedish Whitebeam trees, as tree 2 had only approximately 7 % higher FMC than tree 1. Also, the highest observed FMC in Ash trees was in canopy bottom, while the lowest was in upper canopy, showing significantly different FMC vertical profiles than the hour-glass shaped FMC vertical profiles observed in the Swedish Whitebeam trees.

Holly trees showed the least vertical variation in FMC. Tree 1 had hour-glass shaped FMC vertical profile, with FMC in middle canopy being slightly lower than that in upper and lower canopy. However, tree 2 showed a different behaviour, as FMC in upper and middle canopy was almost constant, while FMC was slightly higher in lower canopy. As discussed in Section 3.2, the vertical variation in FMC within an individual tree can be related to the variation in LMA between the tree layers, as a result of the difference in leaf internal structure and LMA between sun and shade leaves. In addition, the difference in FMC vertical profiles between different trees and/or different species can also be related to the difference in LMA and leaf structure between them. Furthermore, as the plot had a wide canopy gap in the middle, the illumination conditions may be contributing to the variation in FMC between trees, especially those from the same species, as a tree tends to grow sun leaves and shade leaves depending on which regions of canopy are well-lit.

It is worth noting that, due to health and safety workplace constraints, the leaf samples for validation in this study were collected from lower canopy only, and no leaf samples were collected from the upper canopy layers to fully validate the estimated vertical variation of FMC.

4. CONCLUSIONS

This study investigated the potential of using NDI of near- and shortwave-infrared wavelengths, utilized in commercially-available TLS instruments, to generate 3D estimates of FMC. The distribution of FMC within canopy, and how it differs between species and also within each individual species, was studied. In the small tree plot observed in this study, consisting of seven trees from four different species, NDI was found to be moderately correlated to FMC in all four species. However, the NDI – FMC relationship was species-dependant and was influenced by the variation in LMA.

At canopy level, the average error in the FMC estimation was < 5%. The 3D FMC point clouds of all trees in the plot showed some vertical heterogeneity. The vertical distribution of FMC varied between species and also within each species. Although the results obtained in this preliminary study are promising, more experiments that include leaf samples for validation from all canopy layers are needed to validate the accuracy of the 3D FMC estimates. Moreover, transferring the proposed method to a real forest environment would require further investigation into the effects of LMA on the NDI – FMC relationship, and methods to calibrate for such effects will be needed if significant variation in LMA is observed in the forest plot, especially in mixed-species plots.

ACKNOWLEDGEMENTS

The authors would like to thank Hexagon Geosystems for loan of the Leica P50 scanner used in the experiments. The research also made use of equipment funded by UKCRIC - UK Collaboratorium for Research in Infrastructure & Cities: Newcastle Laboratories (EPSRC award EP/R010102/1).

REFERENCES

Ceccato, P., Flasse, S., Tarantola, S., Jacquemoud, S., Grégoire, J.-M., 2001. Detecting vegetation leaf water content using reflectance in the optical domain. Remote sensing of environment 77, 22-33.

Danson, F.M., Bowyer, P., 2004. Estimating live fuel moisture content from remotely sensed reflectance. Remote Sensing of Environment 92, 309-321.

Du, L., Gong, W., Shi, S., Yang, J., Sun, J., Zhu, B., Song, S., 2016. Estimation of rice leaf nitrogen contents based on hyperspectral LIDAR. International Journal of Applied Earth Observation and Geoinformation 44, 136-143.

Eitel, J.U.H., Magney, T.S., Vierling, L.A., Brown, T.T., Huggins, D.R., 2014a. LiDAR based biomass and crop nitrogen estimates for rapid, non-destructive assessment of wheat nitrogen status. Field Crops Research 159, 21-32.

Eitel, J.U.H., Magney, T.S., Vierling, L.A., Dittmar, G., 2014b. Assessment of crop foliar nitrogen using a novel dual-wavelength laser system and implications for conducting laser-based plant physiology. ISPRS Journal of Photogrammetry and Remote Sensing 97, 229-240.

Eitel, J.U.H., Vierling, L.A., Long, D.S., 2010. Simultaneous measurements of plant structure and chlorophyll content in broadleaf saplings with a terrestrial laser scanner. Remote Sensing of Environment 114, 2229-2237.

Eitel, J.U.H., Vierling, L.A., Long, D.S., Hunt, E.R., 2011. Early season remote sensing of wheat nitrogen status using a green scanning laser. Agricultural and Forest Meteorology 151, 1338-1345.

Elsherif, A., Gaulton, R., Mills, J., 2018. Estimation of vegetation water content at leaf and canopy level using dual-wavelength commercial terrestrial laser scanners. Interface Focus 8.

Gaulton, R., Danson, F.M., Ramirez, F.A., Gunawan, O., 2013. The potential of dual-wavelength laser scanning for estimating vegetation moisture content. Remote Sensing of Environment 132, 32-39.

Hakala, T., Nevalainen, O., Kaasalainen, S., Mäkipää, R., 2015. Technical Note: Multispectral lidar time series of pine canopy chlorophyll content. Biogeosciences 12, 1629-1634.

Höfle, B., Pfeifer, N., 2007. Correction of laser scanning intensity data: Data and model-driven approaches. ISPRS Journal of Photogrammetry and Remote Sensing 62, 415-433.

Junttila, S., Sugano, J., Vastaranta, M., Linnakoski, R., Kaartinen, H., Kukko, A., Holopainen, M., Hyyppä, H., Hyyppä, J., 2018. Can Leaf Water Content Be Estimated Using Multispectral Terrestrial Laser Scanning? A Case Study With Norway Spruce Seedlings. Frontiers in plant science 9, 299.

Junttila, S., Vastaranta, M., Liang, X., Kaartinen, H., Kukko, A., Kaasalainen, S., Holopainen, M., Hyyppä, H., Hyyppä, J., 2016. Measuring Leaf Water Content with Dual-Wavelength Intensity Data from Terrestrial Laser Scanners. Remote Sensing 9, 8.

Li, W., Niu, Z., Sun, G., Gao, S., Wu, M., 2016. Deriving backscatter reflective factors from 32-channel full-waveform LiDAR data for the estimation of leaf biochemical contents. Optics Express 24, 4771-4785.

Nelson Jr, R.M., 2001. Water relations of forest fuels, Forest fires. Elsevier, pp. 79-149.

Nevalainen, O., Hakala, T., Suomalainen, J., Mäkipää, R., Peltoniemi, M., Krooks, A., Kaasalainen, S., 2014. Fast and nondestructive method for leaf level chlorophyll estimation using hyperspectral LiDAR. Agricultural and Forest Meteorology 198, 250-258.

Penasa, L., Franceschi, M., Preto, N., Teza, G., Polito, V., 2014. Integration of intensity textures and local geometry descriptors from Terrestrial Laser Scanning to map chert in outcrops. ISPRS Journal of Photogrammetry and Remote Sensing 93, 88–97.

Ramirez, F.A., Armitage, R.P., Danson, F.M., 2013. Testing the application of terrestrial laser scanning to measure forest canopy gap fraction. Remote Sensing 5 (6), 3037–3056.

Riaño, D., Vaughan, P., Chuvieco, E., Zarco-Tejada, P.J., Ustin, S.L., 2005. Estimation of fuel moisture content by inversion of radiative transfer models to simulate equivalent water thickness and dry matter content: Analysis at leaf and canopy level. IEEE Transactions on Geoscience and Remote Sensing 43, 819-826.

Takeda, T., Oguma, H., Sano, T., Yone, Y., Fujinuma, Y., 2008. Estimating the plant area density of a Japanese larch (Larix kaempferi Sarg) plantation using a ground-based laser scanner. Agricultural and Forest Meteorology 148, 428–438.

Valentinuz, O.R., Tollenaar, M., 2004. Vertical Profile of Leaf Senescence During the Grain-filling Period in Older and Newer Maize Hybrids. Crop Science 44, 827–834.

Viegas, D., Viegas, M., Ferreira, A., 1992. Moisture content of fine forest fuels and fire occurrence in central Portugal. International Journal of Wildland Fire 2, 69-86.

Wei, G., Shalei, S., Bo, Z., Shuo, S., Faquan, L., Xuewu, C., 2012. Multi-wavelength canopy LiDAR for remote sensing of vegetation: Design and system performance. ISPRS journal of photogrammetry and remote sensing 69, 1-9.

Yebra, M., Chuvieco, E., Riaño, D., 2008. Estimation of Live Fuel Moisture Content from MODIS Images for Fire Risk Assessment. Agricultural and Forest Meteorology 148, 523−536.

Yilmaz, M.T., Hunt Jr, E.R., Jackson, T.J., 2008. Remote sensing of vegetation water content from equivalent water thickness using satellite imagery. Remote Sensing of Environment 112, 2514-2522.

Zhu, X., Wang, T., Darvishzadeh, R., Skidmore, A.K., Niemann, K.O., 2015. 3D leaf water content mapping using terrestrial laser scanner backscatter intensity with radiometric correction. ISPRS Journal of Photogrammetry and Remote Sensing 110, 14-23.

Zhu, X., Wang, T., Skidmore, A.K., Darvishzadeh, R., Niemann, K.O., Liu, J., 2017. Canopy leaf water content estimated using terrestrial LiDAR. Agricultural and Forest Meteorology 232, 152-162.